HHS Public Access

Author manuscript

J Mech Behav Biomed Mater. Author manuscript; available in PMC 2020 August 01.

Published in final edited form as:

J Mech Behav Biomed Mater. 2019 August ; 96: 204–213. doi:10.1016/j.jmbbm.2019.04.021.

Injectable Cellulose-Based Hydrogels as Nucleus Pulposus Replacements: Assessment of *In Vitro* Structural Stability, *Ex Vivo* Herniation Risk, and *In Vivo* Biocompatibility

Huizi Anna Lin[a], **Devika M. Varma**[a], **Warren W. Hom**[b], **Michelle A. Cruz**[b], **Philip R. Nasser**[b], **Robert G. Phelps**[c], **James C. Iatridis**[b], and **Steven B. Nicoll**[a]

[a]Department of Biomedical Engineering, The City College of New York, New York, NY, USA

[b]Leni & Peter W. May Department of Orthopaedics, Icahn School of Medicine at Mount Sinai, New York, NY, USA

[c]Department of Dermatology and Pathology, Mount Sinai Hospital, New York, NY, USA

Abstract

Current treatments for intervertebral disc degeneration and herniation are palliative only and cannot restore disc structure and function. Nucleus pulposus (NP) replacements are a promising strategy for restoring disc biomechanics and height loss. Cellulose-based hydrogel systems offer potential for NP replacement since they are stable, non-toxic, may be tuned to match NP material properties, and are conducive to cell or drug delivery. A crosslinked, carboxymethylcellulose-methylcellulose dual-polymer hydrogel was recently formulated as an injectable NP replacement that gelled *in situ* and restored disc height and compressive biomechanical properties. The objective of this study was to investigate the translational potential of this hydrogel system by examining the long-term structural stability *in vitro*, the herniation risk and fatigue bending endurance in a bovine motion segment model, and the *in vivo* biocompatibility in a rat subcutaneous pouch model. Results showed that the hydrogels maintained their structural integrity over a 12-week period. AF injury significantly increased herniation risk and reduced fatigue bending endurance in bovine motion segments. Samples repaired with cellulosic hydrogels demonstrated restored height and exhibited herniation risk and fatigue endurance comparable to samples that underwent the current standard treatment of nucleotomy. Lastly, injected hydrogels elicited a minimal foreign body response as determined by analysis of fibrous capsule development and macrophage presence over 12 weeks. Overall, this injectable cellulosic hydrogel system is a promising candidate as an NP substitute. Further assessment and optimization of this cellulosic hydrogel system in an *in vivo* intradiscal injury model may lead to an improved clinical solution for disc degeneration and herniation.

Corresponding author: Steven B. Nicoll, PhD, Department of Biomedical Engineering, The City College of New York, Steinman Hall, Rm 401, 160 Convent Avenue, New York, NY 10031, Phone: 212-650-6237, snicoll@ccny.cuny.edu.

Conflict of interest: none

Keywords

Intervertebral disc; Nucleus pulposus; Injectable hydrogel; Cellulose biomaterial; Herniation risk; Fatigue behavior; Biocompatibility

1. Introduction

Lower back pain is currently the leading cause of disability worldwide (Buchbinder et al., 2013). It is a debilitating health problem with 80–85% lifetime prevalence and incurs substantial socioeconomic burden (Hoy et al., 2010; Katz, 2006). The main contributing factors include intervertebral disc degeneration and disc herniation (Freemont, 2009; Luoma et al., 2000; Schwarzer et al., 1995). The intervertebral disc is a composite, fibrocartilaginous tissue interposed between adjacent vertebral bodies of the spine. Its three distinct components - a gelatinous nucleus pulposus (NP) core surrounded circumferentially by a lamellar annulus fibrosus (AF) and sandwiched superiorly and inferiorly by the cartilaginous endplates – work in conjunction to achieve the disc's vital mechanical function of distributing loads and facilitating flexibility in the spine (Raj, 2008; Whatley and Wen, 2012). Disc degeneration is characterized by loss of proteoglycans in the NP, which leads to reduced hydration, disc height, and intradiscal pressure (Adams and Roughley, 2006; Roughley, 2004; Urban and Roberts, 2003). Additionally, an elevated inflammatory environment and increased mechanical instability have been postulated as sources of pain (Burke et al., 2002; Iatridis et al., 2013; Risbud, 2014). In cases of disc herniation, the AF structural integrity is compromised leading to NP extrusion through the AF (Lasanianos et al., 2015). NP tissue impingement on nerve roots and increased inflammatory cytokines have been implicated in spinal nociception (Aoki et al., 2002; Kang et al., 1996; Olmarker and Rydevik, 1998).

Current treatments for disc degeneration and herniation are only palliative and cannot restore the native disc structure and function. In cases of disc degeneration, spinal fusion is utilized to alleviate pain by stabilizing the entire motion segment. However, this surgery is highly invasive, alters spinal biomechanics, and may even accelerate degeneration in adjacent discs (Lee, 1988; Park et al., 2004). Another treatment is total disc arthroplasty. However, surgery for this treatment is also highly invasive. Furthermore, the properties of these disc replacements do not match that of the native disc, leading to altered disc biomechanics at adjacent levels (Vital and Boissière, 2014). For disc herniation, the most popular treatment is discectomy or nucleotomy, which involves removal of herniated nucleus material. This treatment has many limitations including reduced disc height, altered disc biomechanics, and potential initiation of disc degeneration (Yorimitsu et al., 2001). Additionally, 10–30% of patients experience reherniation, which would necessitate a second nucleotomy procedure and many patients report recurrent pain (Abdu et al., 2017; McGirt et al., 2009; Suk et al., 2001). Thus, current standard treatments for disc degeneration and herniation are inadequate and there exists a pressing need for alternative strategies that can both address pain relief and restoration of native disc biomechanics.

NP replacements have emerged as a promising treatment for disc herniation and early disc degeneration in cases where the annulus is still competent (Di Martino et al., 2005; Goins et al., 2005; Lewis, 2012). A careful screening and evaluation process for NP replacement materials involves optimization tests that screen multiple formulations, *in situ* validation tests of increasing complexity, and further evaluations using *in vivo* pre-clinical models in advance of eventual human trials (Long et al., 2016b). An ideal nucleus implant would be injectable to facilitate a minimally invasive procedure, match the material properties of healthy native NP, reestablish disc height and impede the progression of degeneration, restore disc mechanical function without compromising herniation risk, and exhibit good biocompatibility (Bowles and Setton, 2017). Hydrogels are ideal candidates as they can be formulated to be injectable and mimic the mechanical properties of the native NP tissue. As such, development of injectable hydrogels for NP implantation and functional restoration of spine biomechanics is an active area of research. For example, Balkovec et al. investigated the ability of a poly(N-isopropylacrylamide and poly(ethylene glycol) composite hydrogel for restoring angular stiffness of porcine motion segments (Balkovec et al., 2013). Cannella et al. assessed the compressive mechanical behavior of human discs after injection of a hydrogel system composed of polyvinyl alcohol and polyvinyl pyrrolidone (Cannella et al., 2014). Li et al. evaluated the compressive performance of a polyurethane scaffold in bovine motion segments (Li et al., 2016), and Smith, Showalter, and Gullbrand et al. extensively examined the biomechanical performance of a triple-interpenetrating-network gel consisting of dextran, chitosan, and teleostean (Gullbrand et al., 2017; Showalter et al., 2015; Smith et al., 2014). Some of these hydrogel formulations require several hours of curing time or complex preparation (freeze-thaw cycles), which may be less amenable to clinical translation (Cannella et al., 2014; Smith et al., 2014). Additionally, general shortcomings associated with the use of synthetic materials for musculoskeletal tissue engineering applications include biological incompatibility and release of unfavorable byproducts (O'Brien, 2011).

An injectable cellulose-based hydrogel system was recently developed and shown to be a promising candidate for NP replacement that can address the limitations associated with the aforementioned synthetic scaffolds (Varma et al., 2018a). This hydrogel system consists of two cellulose derivatives – carboxymethylcellulose (CMC) and methylcellulose (MC), both of which are further advantageous in that they are plant-based and low-cost, have an extensive safety profile with the FDA, and can provide long-term stability by avoiding enzymatic degradation in the human body. Additionally, each polymer has its own unique features contributing to the development of an injectable NP replacement. CMC has a high capacity for water uptake due to the carboxyl groups along the polymer backbone, akin to the highly negatively-charged, proteoglycan-rich extracellular matrix of the native NP tissue (Gupta et al., 2011; Reza and Nicoll, 2010). Previous studies have demonstrated that CMC hydrogels possess similar material properties as the native NP, and are capable of supporting NP cell-like differentiation of encapsulated human mesenchymal stem cells (Gupta et al., 2011; Lin et al., 2016). MC exhibits intrinsic thermogelation above 32°C (Haque and Morris, 1993), which increases the viscosity of the polymer solution at body temperature and facilitates *in situ* gelation (Nasatto et al., 2015; Varma et al., 2018a). The injectability and gelation of CMC-MC hydrogels is achieved by modifying both cellulosic polymers with

methacrylate groups that allow for radical polymerization when employing a redox-initiated crosslinking mechanism (Reza and Nicoll, 2010; Varma et al., 2018a). A recent study demonstrated that CMC-MC hydrogels were able to gel *in situ* in bovine motion segments and restore disc height and biomechanical parameters in axial compression post-nucleotomy (Varma et al., 2018a). Although the results are encouraging, as with other hydrogel systems, several concerns must be addressed before clinical translation of these hydrogels is realized, such as long-term structural stability, response under rigorous biomechanical evaluations, and *in vivo* foreign body reaction.

In order to evaluate the clinical potential of CMC-MC hydrogels as NP replacements, the overall objective of this study was to assess key performance characteristics including long-term structural integrity, herniation risk, behavior under fatigue bending, and *in vivo* biocompatibility. Degradation characteristics and associated long-term structural longevity are important factors for acellular nucleus replacements. Herniation risk is a crucial parameter to examine as most NP implants have failed due to extrusion (Di Martino et al., 2005; Lewis, 2012). An excellent herniation test has been developed to measure failure strength *in situ*, in which the amount of force required to produce herniation is simulated in order to determine whether the injected biomaterial can withstand physiological loading conditions (Vergroesen et al., 2015). Fatigue bending behavior is another critical outcome measure, as a successful NP substitute must endure many cycles of eccentric compressive loading in the spinal unit, and the most rigorous test for fatigue bending was developed by Wilke and co-authors (Wilke et al., 2013). Lastly, *in vivo* biocompatibility is essential for an NP replacement, since an injectable material would need to be tolerated by the body. For a novel hydrogel biomaterial, the local histopathological response should be assessed following hydrogel injection in accordance with the ISO standard for biological evaluation for medical devices.

2. Materials and Methods

2.1. Polymer synthesis

Methacrylation of CMC and MC (Sigma-Aldrich, St. Louis, MO) polymer was performed as described previously (Reza and Nicoll, 2010). 90 kDa CMC and a 1:1 mix of 14 kDa and 41 kDa MC were used. Briefly, a 1% (w/v) solution of CMC or MC was reacted with a 40-fold excess of methacrylic anhydride (Sigma) in deionized water at 4°C and a pH of 8.0 for over 24 hrs. The modified polymer solution was then purified via dialysis for 72 hrs to remove unreacted methacrylic anhydride. Lastly, the purified, modified polymer was recovered via lyophilization and the solid product was stored at −20°C. The degree of methacrylation was determined using ^{1}H-NMR (300 MHz, Varian Mercury 300, Agilent Technologies) on acid hydrolyzed samples. Methacrylation percentage was quantified by the relative integrations of methacrylate proton peaks (methyl peak, $\delta \sim 2.0$ ppm; methylene peaks, $\delta \sim 5.8$ and 6.2 ppm) to carbohydrate protons. CMC with methacrylation percentage of ~15% and MC with methacrylation percentage of ~10% were employed in this study.

2.2. Hydrogel preparation

The formulation of CMC-MC used in this study was optimized in a previous investigation (Varma et al., 2018a). Methacrylated CMC and MC, dissolved in phosphate-buffered saline (PBS) (Sigma-Aldrich) at 3% (w/v) macromer concentration each, were homogeneously combined in both barrels of dual-barrel syringes (Pac-Dent, Brea, CA). Redox initiators, ammonium persulfate (APS) (Sigma-Aldrich) and N,N,N',N'-tetramethylethylenediamine (TEMED) (Fisher Scientific, Hampton, NH) were added to the separate barrels of the syringes at 20 mM each and mixed with the polymer solution. Trypan Blue (Fisher Scientific) was added to the polymer solution as well to facilitate enhanced visual detection of the hydrogel post gelation. Following a 30-min incubation period in a 37°C water bath to initiate MC gelation, the polymer mixtures were injected via a 20G needle (Fisher Scientific) attached to a mixing tip (Pac-Dent) connected to the syringe (Figure 1A)

2.3. In vitro structural stability

In vitro structural stability of CMC-MC hydrogels was determined by examining the shape, dry weight, and mechanical properties of hydrogels over a 12-week period. Hydrogels, 5 mm in diameter and 2 mm in thickness, were fabricated in a custom casting mold (Chou and Nicoll, 2009). Samples were then incubated in PBS at 37°C on an orbital shaker for the duration of the experiment in order to best mimic the temperature and fluid flow of the native disc environment. Imaging and unconfined compression testing was performed on gels after 1 day (D1), 2 weeks (Wk2), 4 weeks (Wk4), 8 weeks (Wk8), and 12 weeks (Wk12) of incubation ($n = 9$). Images of the hydrogels were captured using a Zeiss Stemi 2000-c stereomicroscope. Testing was conducted using a custom-built apparatus as described in previous studies (Chou and Nicoll, 2009; Reza and Nicoll, 2010). The testing protocol consisted of a creep tare test and a multi-ramp stress-relaxation test. During the creep test, a 1.0-g tare load was applied to the hydrogel at a ramp velocity of 10 μm/s for 1800 s until equilibrium was reached. During the multi-ramp stress-relaxation test, three 5% strain ramps were applied to the hydrogel at a ramp velocity of 10 μm/s, each followed by a 2000-s relaxation period. Equilibrium stress was calculated and plotted against the applied strain for each ramp. An average equilibrium Young's Modulus was determined from the slope of the stress versus strain curve. After mechanical testing, the gels were lyophilized and the dry weight was obtained by measurement using an analytical balance.

2.4. Motion segment preparation

Vertebrae-disc-vertebrae motion segments (cc1–2, cc2–3, and cc3–4) were harvested from healthy, skeletally mature bovine tails (Green Village Packing, Green Village, NJ). All facet and transverse processes, along with extraneous musculature and ligaments, were carefully removed to preclude their contribution to disc mechanics. Resulting samples were frozen at −20°C for 2–3 weeks until testing, based on prior studies using ovine and human motion segments, which showed no significant effect of a single freeze-thaw cycle on intervertebral disc mechanical properties (Smeathers and Joanes, 1988; Gleizes et al., 1998; Dhillon et al., 2001).

2.5. Evaluation of herniation risk

Bovine coccygeal motion segments were isolated by sawing parallel cuts through the vertebral bodies approximately 3 mm from the edge of the disc. Samples were thawed in PBS at room temperature for 2 hrs prior to specimen preparation. Motion segments were evenly distributed into four groups (n = 12/group): (1) Intact, (2) Injury, (3) Nucleotomy, and (4) CMC-MC Repair. The Intact specimens did not undergo any further preparation. For Injury specimens, a cruciate incision at the posterolateral region of the annulus was created with a #15 blade and the NP was disrupted with a curette to simulate the clinical condition of an AF injury. For Nucleotomy specimens, approximately 0.15 – 0.20 g of NP (~50–80% of the total NP weight) was removed using a pituitary rongeur following AF incision to mimic the clinical standard treatment of nucleotomy. Lastly, for Repair specimens, CMC-MC solutions were injected into the NP void of nucleotomized specimens using dual-barrel syringes with a 20G needle and then samples were incubated at 37°C for 30 min to facilitate complete gelation of the hydrogels. All specimens were left in PBS with protease inhibitor (Roche Diagnostics, Indianapolis, IN) at 4°C overnight before testing the next day. Herniation risk was evaluated through failure testing using a MTS Bionix Servohydraulic Test System (MTS, Eden Parairie, MN). Specimens were placed on the MTS stage at an offset of 5° from the normal axis, with the postero-lateral portion of the disc at the outside of the bend to simulate postero-lateral flexion. A force of ~20 N was applied as a pre-load. The samples were then compressed in displacement-control mode using a ramp function at 2 mm/min until failure (Figure 1B). Force-displacement curves were obtained and analyzed using custom MATLAB (Mathworks, Natick, MA) code. Video recordings of the tests were obtained as well. Failure was defined by either endplate fracture, as indicated on the force-displacement curves, or by significant NP or CMC-MC protrusion greater than 2 mm, as indicated from both the force-displacement curves and visually from the video recordings. Failure strength was calculated as the load at failure normalized to the disc area. Subsidence-to-failure was determined by the displacement curve prior to the failure point. Maximum stiffness was calculated as the maximum value of force divided by displacement before the failure point. Work-to-failure was determined from the area under the force-displacement curve before the failure point.

2.6. Assessment of fatigue endurance

Fatigue endurance was determined using a fatigue loading protocol adapted from Wilke et al. (Ordway et al., 2013; Wilke et al., 2013). Bovine motion segments were thawed in PBS at room temperature for 2 hrs then potted in poly(methyl methacrylate) prior to specimen preparation as described previously (Long et al., 2016a; Varma et al., 2018a). Similar to failure testing, bovine motion segments were evenly distributed into four groups (n = 9/group): (1) Intact, (2) Injury, (3) Nucleotomy, and (4) CMC-MC Repair. Prepared specimens were incubated in PBS with protease inhibitor at 4°C overnight. On the following day, the fatigue bending tests were conducted at room temperature with specimens hydrated with PBS during the entirety of the tests. The fatigue loading protocol consisted of cyclic eccentric compression between 50N and 300N at 1 Hz and at an offset of 20 mm to induce a physiological bending moment of 6 Nm (Figure 1C & 1D). The loading indenter cyclically rotated from −135° to +135° from the axis opposite of the incision site at 15° increments with 1 min of cyclic loading at each location. This test setup was considered to mimic the

"worst-case scenario" as loading opposite of the injury site was expected to aggravate NP or CMC-MC extrusion. Failure was defined by significant NP or CMC-MC protrusion greater than 2 mm. The main outcome measure from the fatigue tests was cycles-to-failure, which was indicative of fatigue endurance.

2.7. Disc height analysis

The specimens used for disc height measurements were from the fatigue testing samples (n = 9). X-rays were taken during sample preparation, before mechanical testing. Motion segments in the Nucleotomy group underwent X-ray imaging in their intact and nucleotomized conditions. Motion segments in the Repair group underwent X-ray imaging in their intact, nucleotomized, and repaired conditions. From the digital X-ray radiographs, the top and bottom endplates of each sample were traced using ImageJ (NIH, Bethesda, MD). The average disc height was then determined using a custom MATLAB code.

2.8. In vivo biocompatibility

The foreign body response to CMC-MC hydrogels was examined over 12 weeks in a rat subcutaneous pouch model ($n = 9$). This testing method, including type of animal, number of samples, evaluation methods, and duration of the study were chosen based on ISO-10933–6 guidelines for "Biological evaluation for medical devices – tests for local effects after implantation." The biological response was generally determined by assessing the macroscopic and histopathological responses over time. Specifically, fibrous capsule development around the hydrogel and local macrophage presence were examined using both quantitative and semi-quantitative measures as described in the ISO standard. The subcutaneous pouch model has been commonly used for initial assessment of the biological safety of new materials (Ibim et al., 1998; Subramanian et al., 2013). All procedures were performed in compliance with a protocol approved by the City College of New York Institutional Animal Care and Use Committee.

2.8.1. Hydrogel injections—Male Sprague-Dawley rats (n=9) (Charles River Laboratories, Kingston, NY) weighing 200 – 250 g (6–8 weeks old) were used. Hydrogel preparation was similar to that described earlier, with the addition of UV-sterilization of CMC and MC polymer and filter-sterilization of redox initiators prior to usage. Approximately 500 μL of CMC-MC hydrogel solutions were injected into the subcutaneous dorsa with 20G needles while the rats were under isoflurane-O_2 general anesthesia. The rats remained under anesthesia for 30 min after injection to ensure complete gelation of the polymer solution. Rats were then transferred back to their cages and periodically monitored for infection at the injection sites and change in overall behavior. Gels were injected 1 week, 4 weeks, and 12 weeks prior to gel extraction.

2.8.2. Hydrogel extractions, processing, and embedding—Injected hydrogels were harvested after the rats were sacrificed by CO_2 asphyxiation. The gels, along with any surrounding fibrous capsule, were extracted using a tweezer and scalpel. The isolated hydrogels were first rinsed in PBS and then fixed in zinc-buffered formalin (Z-fix) (Anatech, Battle Creek, MI) for 48 hrs. Fixed gels were next processed in ethylene glycol monoethyl ether (EGME) (Fisher Scientific), dehydrated in a graded series of ethanol, and then

embedded in paraffin. Embedded gels were sectioned to a thickness of 8 μm using a Thermo Scientific Rotary Microtome (Model HC325, Walldorf, Germany).

2.8.3. Histological and immunohistochemical evaluations—Sample sections were deparaffinized using CitriSolv (Fisher Scientific) followed by rehydration in a graded series of ethanol. Following hydration, the sections were then stained with Hematoxylin and Eosin (Sigma) to visualize cell and tissue morphology and distribution. Three measurements of fibrous capsule thickness were obtained by a histopathologist for each sample using a calibrated eyepiece reticle in order to calculate an average value per sample. Macrophage presence was examined using immunohistochemical staining with a mouse anti-CD68 antibody (Abcam, Cambridge, United Kingdom) in conjunction with a peroxidase-based detection system using 3,3'-diaminobenzidine chromogen (Vector Labs, Burlingame, CA). Toluidine Blue (Sigma) staining was used to detect the gel. Sample sections incubated with non-immune IgG (Sigma) instead of CD68 antibody served as negative controls, sections of skin sample served as naïve controls, and sections of spleen served as positive controls. Severity of macrophage presence was graded by a histopathologist using the guideline of "+" indicating mild, "++" moderate, and "+++" severe response, with blind assessment. Slides were viewed with a Zeiss Axio Imager Z1 (Carl Zeiss, Oberkochen, Germany) optical microscope and images were captured using AxioVision software (Carl Zeiss).

2.9. Statistical analysis

A Shapiro-Wilk test was performed to determine the normality of the data sets. Due to the normality of the *in vitro* structural stability and motion segment failure testing data sets, a one-way ANOVA with Tukey's post-hoc test was used to compare values of gel dry weight, hydrogel equilibrium modulus, failure strengths, subsidence-to-failure, maximum stiffness, and work-to-failure. Due to the non-Gaussian distribution of the fatigue testing data set, a Kruskal-Wallis (non-parametric one-way ANOVA) with Dunn's Multiple Comparison test was used to compare values of cycles-to-failure. Due to the normality of the fibrous capsule thickness data set, one-way ANOVA with Tukey's post-hoc test was used to compare values across time points. Data are represented as mean ± standard deviation for all analyses. Significance was set at $p < 0.05$. All statistical analyses were performed using GraphPad Prism v.5 (GraphPad Software, San Diego, California).

3. Results

3.1 In vitro structural stability

In vitro structural stability of CMC-MC hydrogels was determined by qualitative assessment of the shape and by quantitative examination of the material properties of the hydrogels after PBS incubation. The hydrogel shape appeared to remain similar during the 12-week study, with no noticeable changes in dimensions (Figure 2A). The mass and the mechanical stiffness of the hydrogels were also maintained throughout the 12-week period (Figure 2B–C). Specifically, there was no significant difference in dry weight among samples at the various time points (D1: 2.3 ± 0.5 mg; Wk2: 2.2 ± 0.2 mg; Wk4: 2.1 ± 0.2 mg; Wk8: 2.2 ± 0.3 mg; Wk12: 2.1 ± 0.4 mg). Likewise, equilibrium Young's modulus values were not

significantly different over the duration of the study (D1: 35.9 ± 6.4 kPa; Wk2: 37.8 ± 4.6 kPa; Wk4: 35.4 ± 8.7 kPa; Wk8: 36.5 ± 8.9 kPa; Wk12: 35.4 ± 6.6 kPa).

3.2. Herniation risk

Herniation risk of CMC-MC hydrogels was assessed through failure testing using a bovine motion segment model. All Intact samples failed by endplate fracture whereas all other samples failed by nuclear extrusion, as indicated by their force-displacement curves and from visual confirmation (Figure 3). The failure strengths of Injury specimens (2.2 ± 2.0 MPa) and Nucleotomy samples (7.0 ± 4.1 MPa) were significantly lower than those of the Intact group (13.0 ± 3.9 MPa) (Figure 4A). Values for the CMC-MC Repair group (9.7 ± 2.1 MPa) were significantly higher than those of the Injury group, but not significantly different from the Intact or Nucleotomy group. Subsidence-to-failure (Intact: 4.0 ± 0.9 mm; Injury: 1.5 ± 0.7 mm; Nucleotomy: 2.8 ± 0.9 mm; CMC-MC Repair: 3.7 ± 0.6 mm), maximum stiffness (Intact: 1.52 ± 0.35 kN/mm; Injury: 0.50 ± 0.35 kN/mm; Nucleotomy: 0.95 ± 0.41 kN/mm; CMC-MC Repair: 1.18 ± 0.23 kN/mm), and work-to-failure (Intact: 8.5 ± 4.9 J; Injury: 0.7 ± 0.8 J; Nucleotomy: 3.0 ± 2.3 J; CMC-MC Repair: 5.1 ± 2.0 J) shared similar trends as those of failure strength (Figure 4B–D). In summary, annulus injury significantly increased herniation risk compared to Intact samples. Nucleotomy and CMC-MC Repair groups displayed reduced herniation risk compared to the Injury group, and were not significantly different from each other. However, unlike the Nucleotomy group, the CMC-MC Repair group was not significantly different from the Intact group in terms of failure strength, maximum stiffness and subsidence to failure.

3.3. Fatigue behavior

Fatigue endurance of CMC-MC hydrogels was evaluated utilizing a fatigue bending testing protocol in a bovine motion segment model. Intact specimens did not fail during test of 21,000 cycles. The Injury group exhibited low fatigue endurance, failing after 1,470 ± 1830 cycles (Figure 5). Nucleotomy and CMC-MC Repair samples (7410 ± 4710 cycles and 7890 ± 5010 cycles, respectively) demonstrated higher fatigue endurance compared to the Injury group, and were not significantly different from each other. Measurements of disc height from x-ray radiographs revealed that nucleotomy reduced disc height to 89.4 ± 4.3% of intact height, and CMC-MC was able to restore disc height to 101.0 ± 3.4% of the intact height.

3.4. In vivo biocompatibility

In vivo biocompatibility of CMC-MC hydrogels was examined using a rat subcutaneous pouch model. The structural integrity of all gels was maintained over the implantation period of 12 weeks (Figure 6A–B). The foreign body response at week 1 was mainly characterized by histiocytes lining the implant surface (Figure 6C). At week 4, there was some subsidence of the histiocytic reaction and initial development of fibrous capsules. By week 12, there was a resolution of the histiocytic reaction, clear evidence of aligned, laminated fibrous capsules, and some gel degradation. Due to the fact that the CMC-MC hydrogels were crosslinked *in vivo*, fibrous capsule formation was variable and inconsistent around the gels. Average fibrous capsule thicknesses were not significantly different across the three time points (Week 1: 70.7 ± 24.1 μm; Week 4: 48.6 ± 13.2 μm; Week 12: 80.6 ± 39.1 μm) (Figure 6D).

The histiocytic reaction was further characterized by CD68 immunostaining. Moderate macrophage presence was detected at week 1, which subsided by week 12 (Figure 7). No severe adverse responses were observed, such as tissue necrosis, thick and increasing fibrous capsule formation, or chronic presence of foreign body giant cells. Overall, CMC-MC hydrogels elicited a minimal foreign body reaction in a vascularized environment.

4. Discussion

There is a critical need for injectable NP replacements since existing treatments do not repair degenerated and injured intervertebral discs following herniation or degeneration (Di Martino et al., 2005; Goins et al., 2005; Lewis, 2012). An *in situ* gelling cellulosic hydrogel was previously developed and shown to restore disc height and compressive disc mechanics in a bovine motion segment model (Varma et al., 2018a). However, critical translational potential of this, and other, hydrogel systems requires assessments of long-term stability and capacity to resist herniation. As such, the current investigation specifically evaluated the *in vitro* stability, herniation risk, fatigue endurance under bending, and *in vivo* biocompatibility of this cellulosic hydrogel system. Overall, CMC-MC hydrogels demonstrated structural longevity, disc height restoration, comparable herniation risk and fatigue endurance compared to the current treatment, and good *in vivo* biocompatibility.

Long-term structural integrity is an important consideration for acellular nucleus replacements. Implanted hydrogels are usually susceptible to two types of degradation – hydrolytic and enzymatic. In this study, *in vitro* hydrolysis was examined. Results revealed that there was no noticeable change in shape and no significant difference in equilibrium moduli of CMC-MC hydrogels over a 12-week incubation period. The maintenance of structural stability by the CMC-MC hydrogels can be attributed to the high polymer content (6% (w/v) equivalent), robust redox-initiated crosslinking, and the hydrophobicity of MC (Nasatto et al., 2015). It should be noted that the unconfined compression tests to measure the equilibrium mechanical properties of the CMC-MC hydrogels do not adequately capture the non-linear behavior of the viscoelastic materials. However, the equilibrium states of the multi-ramp stress-relaxation tests can be approximated as linear in order to obtain the equilibrium Young's moduli of the gels (as evidenced by R^2 values of close to 0.95, which suggest a good linear fit of the data in the stress-strain curves). Although enzymatic degradation was not directly assessed in this study, CMC-MC should fare well *in vivo* considering that humans lack cellulase. This characteristic favors the longevity of implanted CMC-MC hydrogels. In this regard, cellulose-based materials possess a key advantage over many existing natural biopolymers (i.e., hyaluronic acid, collagen) being explored for NP tissue replacements. Nevertheless, in order to move closer to clinical translation, it would be necessary to perform degradation studies in an *ex vivo* motion segment model under more physiologic conditions (i.e., mechanical, biochemical). Aside from biomechanical outcome measures, hydrogel morphology could be evaluated using imaging techniques, and spectroscopic analytical methods could be employed to characterize the degradation products.

Selection of appropriate models for mechanical and biocompatibility testing is crucial. This study utilized a bovine motion segment model for the biomechanical assessments and a rat

subcutaneous pouch model for evaluation of *in vivo* biocompatibility. Bovine motion segments are a suitable model choice for biomechanical evaluation of NP implants as their discs are large in size and possess properties comparable to human lumbar IVDs (Beckstein et al., 2008; Demers et al., 2004; O'Connell et al., 2007; Oshima et al., 1993; Showalter et al., 2012). Furthermore, they are easily obtainable and well-investigated in the disc field (Likhitpanichkul et al., 2014; Roberts et al., 2008; Walter et al., 2014). The experimental groups in the study were designed to mimic clinically-relevant scenarios. For example, the Injury group simulated the scenario of an AF injury with loose NP material that herniates under relatively low forces. The Nucleotomy group mimicked the current standard treatment of discectomy which removes all loose NP material without repairing the AF defect. The amount of NP removal generally varies case by case in the clinical setting, however, the amount removed in this study was maintained within the same range of 0.15 – 0.20 g in order to minimize variability and for comparison to other studies (Long et al., 2016a; Showalter et al., 2014). Moreover, this nucleotomy model produced losses in disc height comparable to values reported following clinical discectomy procedures (McGirt et al., 2009). It should also be acknowledged that since the amount of tissue removed is based on human clinical practice, the model likely represents a more extreme case given the difference in geometry between the human and bovine disc (O'Connell et al., 2007). For assessment of *in vivo* biocompatibility, the rat subcutaneous pouch model is a standard model for initial evaluation of biomaterial biocompatibility as it is simple, easily accessible, and inexpensive (ISO-10993–6, 2008; Kastellorizios et al., 2015; Onuki et al., 2008). The highly vascularized environment of the subcutaneous pouch is suitable for examining the biological response to implanted materials. Although this environment is different from the one where the NP replacement will be applied, the NP tissue is immune-privileged, and therefore, should result in a lesser degree of foreign body reaction (Raj, 2008; Risbud, 2014; Whatley and Wen, 2012).

This study confirmed the ability for CMC-MC hydrogels to undergo *in situ* gelation and restore disc height loss due to nucleotomy. The thermogelation property of MC enables *in situ* gelation at the injection site whereas the hydrophilicity of the polyanionic CMC macromolecule imparts greater swelling capability. Hydrogel injectability is an important feature for facilitating a minimally-invasive restorative procedure. This feature presents an improvement over the first generation of preformed NP replacements (Di Martino et al., 2005; Lewis, 2012). *In situ* gelation also allows the resulting hydrogel to conform to the NP void space and integrate better with the native tissue. Additionally, the previously measured gelation time for CMC-MC hydrogels was ~4 minutes (Varma et al., 2018a), which is within the 4–15 minute window suggested by ISO standard 5833/1–999E for injectable materials, and represents an advantage over other hydrogel systems that require longer curing time (Smith et al., 2014). Lastly, the ability of CMC-MC hydrogels to restore disc height is critical, as disc height is an important clinical parameter and restoration can decelerate disease progression (Griffith et al., 2007; Pfirrmann et al., 2001; Schnake et al., 2006). Despite the demonstrated advantages of this hydrogel system, the motion segments were not subjected to a compressive preload during injection, which differs from the clinical scenario. Therefore, the observed *in situ* gelation might not be as effective in a surgical setting in

which resistive compressive loads are experienced, warranting the application of a preload in future studies utilizing this injury model.

Herniation risk is another crucial factor for NP implants. The herniation risk of CMC-MC hydrogels was evaluated through failure testing. The test was conducted in compression with 5° posterolateral flexion exposing the annulus injury site, as compression with flexion simulates the main mode of failure experienced by discs (Adams and Hutton, 1981; Wilke et al., 2013). The failure test was clinically relevant as it provided insight into the maximum strength and displacement that can be sustained before the specimens herniate (Long et al., 2017; Vergroesen et al., 2015). The test also provided both the maximum stiffness exhibited by the disc and the energy required before failure, as indicated by the work-to-failure parameter. Overall, AF injury significantly increased herniation risk, which was expected as the main role of the AF is to resist tension and maintain disc shape. The values obtained for Intact, Injury, and Nucleotomy are comparable to those reported in the literature (Long et al., 2017; Vergroesen et al., 2015). Injury specimens exhibited the highest herniation risk, which can be attributed to the combination of high intradiscal pressure, abundant NP tissue, and a large cruciate injury. Nucleotomy samples were still susceptible to reherniation due to the swelling of residual NP tissue and the unrepaired AF. CMC-MC Repair demonstrated comparable performance to Nucleotomy, which simulated the current clinical treatment. Still, it is important to highlight the fact that the CMC-MC Repair group was not significantly different from the Intact group with respect to most of the measured failure properties (i.e., failure strength, maximum stiffness and subsidence to failure), in contrast to the Nucleotomy specimens. This result may be due to the restored disc hydration by the hydrogels without substantial sealing of the AF injury.

A successful NP replacement would need to withstand many cycles of loading in the *in vivo* environment, thus fatigue testing was utilized to assess the fatigue endurance of CMC-MC hydrogels. The fatigue loading protocol used in this study was adapted from a testing regime utilized by Wilke et al., which has become a standard for rigorous testing of disc repair implants (Wilke et al., 2013). The eccentric compression mode at locations opposite of the AF injury site was intended to simulate bending loading modes that would aggravate NP herniation or implant extrusion, and is therefore, considered a rigorous loading regime. Furthermore, the loading frequency of 1 Hz is within the physiological range of 0.5 – 2 Hz (Neidlinger-Wilke et al., 2014). Lastly, when normalized by the cross sectional area, the bending moment of 6 Nm used in this study for bovine discs is comparable to the ISO standard of 10–12 Nm for total disc replacement evaluation in human discs (O'Connell et al., 2007; Wilke et al., 2013). This normalized bending moment would still represent the high end of the physiological range, and thus, is an appropriate value to use. Similar to the results from failure testing, AF injury significantly decreased fatigue endurance of specimens. The Injury group exhibited very low fatigue endurance (~1,500 cycles). Nucleotomy (~7,400 cycles) and CMC-MC Repair (~7,900 cycles) demonstrated higher fatigue endurance compared to the Injury group but were comparable to each other. It is difficult to directly compare the performance of CMC-MC hydrogels to others reported in literature as testing protocols differ among studies. For example, although the Barricaid device in Wilke's study drastically reduced herniation risk, the implant required invasive surgical procedures and was intended as an AF closure (Wilke et al., 2013). Several studies

reported higher fatigue endurance for other nucleus implants, however, testing was done in a direct axial compression mode, and as such, represents a less rigorous testing condition (Schmocker et al., 2016; Vergroesen et al., 2015). Balkovec et al. tested a PEG-based hydrogel in flexion-extension mode, but only up to 8,000 cycles (Balkovec et al., 2013). Ordway et al. tested a synthetic NP substitute in an eccentric compression mode similar to this study, but the bending moment used was 2.5–7.5 Nm for a human motion segment, which is less demanding than that used in this study (Ordway et al., 2013). Therefore, the fatigue protocol developed in this study represents a rigorous test suitable for evaluation of implants in bovine motion segments. Based on an estimate that the average person experiences 125,000 "significant bends" in flexion/extension per year (Hedman et al., 1991), the Nucleotomy and CMC-MC Repair samples would be expected to fail after 3–4 weeks *in vivo*. Nevertheless, actual failure would be dependent on the specific loading parameters (i.e., bending moment), and the values selected for this study were on the high end of the physiological range. Moreover, the test setup was considered to mimic the "worst-case scenario," as loading opposite of the injury site was expected to be more conducive to NP or CMC-MC extrusion. Hence, under normal physiologic loading conditions, the hydrogel implant would likely remain intact for longer than 3–4 weeks.

Any new biomaterial requires assessment of *in vivo* biocompatibility. The ISO standard is an important assessment to inform the size of the fibrous capsule and inflammatory foreign body response expected for implantation of any biomaterial. Although CMC and MC individually have been established as biocompatible polymers (Miyamoto et al., 1989), long-term *in vivo* biocompatibility of this redox-initiated CMC-MC hydrogel system had not been investigated. The fibrous capsule formation around the CMC-MC hydrogels observed in this study represents a normal and mild foreign body response (Kastellorizios et al., 2015). Capsule thickness remained within 35–120 μm over a 3-month period, indicating a mild response comparable to other biomaterials used for biomedical applications (Bongio et al., 2013; Deng et al., 2010). Macrophage presence subsided from week 1 to week 12, further supporting the biological safety of the injected cellulosic hydrogels. Taken together, CMC-MC hydrogels elicited a minimal foreign body response in a vascularized environment. Although a similar or milder response would be expected in the avascular, immune-privileged disc environment, future examination is necessary to confirm this hypothesis (Raj, 2008; Risbud, 2014; Whatley and Wen, 2012).

Overall, this study demonstrated that CMC-MC is a promising NP replacement material that improves IVD biomechanics and exhibits good *in vitro* structural stability and *in vivo* biocompatibility without increasing herniation risk as compared to the current clinical treatment (i.e., nucleotomy). In order to further reduce the herniation risk and increase fatigue endurance, additional improvements to hydrogel retention could be made by enhancing hydrogel adhesion, by incorporating the use of an annulus sealant, or by adding an AF closure device in order to reduce or eliminate herniation risk (Balakrishnan et al., 2017; Charron et al., 2016; Cruz et al., 2018; Likhitpanichkul et al., 2014; Long et al., 2017; Parker et al., 2016). Future investigations will also include *in vivo* testing of these cellulosic hydrogels in the intradiscal space of large animals, for assessment of biomechanical restoration and biocompatibility in a more representative model. In addition, the materials may be employed as delivery vehicles for biological agents such as soluble growth factors

and stems cells to aid in the repair process and improve functional outcomes, as described in a recent study using injectable, redox-polymerized CMC gels for encapsulation of human marrow-derived stromal cells *in vitro* (Varma et al., 2018b).

5. Conclusion

The translational potential of an injectable cellulosic hydrogel system was investigated in this study. Results demonstrated that CMC-MC hydrogels can gel *in situ* and restore disc height without compromising herniation risk compared to the current clinical treatment of nucleotomy. CMC-MC hydrogels maintained long-term structural stability *in vitro* and exhibited good *in vivo* biocompatibility in a rodent subcutaneous pouch model. Future work will focus on further enhancing hydrogel retention and investigating hydrogel performance in an *in vivo* disc injury model. Successful development of an injectable NP replacement will be beneficial for many patients suffering from disc herniation and degeneration.

Acknowledgements

This work was funded by NIH NIAMS R01AR057397 (J.C.I.) and NSF IIP 1701120 (S.B.N.). The authors thank Damien Laudier, Dr. Gittel Gold, and Kevin Seon of CCNY for technical assistance.

References

Abdu RW, Abdu WA, Pearson AM, Zhao W, Lurie JD, Weinstein JN, 2017 Reoperation for Recurrent Intervertebral Disc Herniation in the Spine Patient Outcomes Research Trial. Spine (Phila. Pa. 1976). 42, 1106–1114. 10.1097/BRS.0000000000002088 [PubMed: 28146015]

Adams MA, Hutton WC, n.d. Prolapsed intervertebral disc. A hyperflexion injury 1981 Volvo Award in Basic Science. Spine (Phila. Pa. 1976). 7, 184–91.

Adams MA, Roughley PJ, 2006 What is intervertebral disc degeneration, and what causes it? Spine (Phila. Pa. 1976). 31, 2151–61. 10.1097/01.brs.0000231761.73859.2c [PubMed: 16915105]

Aoki Y, Rydevik B, Kikuchi S, Olmarker K, 2002 Local application of disc-related cytokines on spinal nerve roots. Spine (Phila. Pa. 1976). 27, 1614–7. [PubMed: 12163720]

Balakrishnan B, Soman D, Payanam U, Laurent A, Labarre D, Jayakrishnan A, 2017 A novel injectable tissue adhesive based on oxidized dextran and chitosan. Acta Biomater. 53, 343–354. 10.1016/j.actbio.2017.01.065 [PubMed: 28131944]

Balkovec C, Vernengo J, McGill SM, 2013 The use of a novel injectable hydrogel nucleus pulposus replacement in restoring the mechanical properties of cyclically fatigued porcine intervertebral discs. J. Biomech. Eng 135, 61004–5. 10.1115/1.4024285 [PubMed: 23699716]

Beckstein JC, Sen S, Schaer TP, Vresilovic EJ, Elliott DM, 2008 Comparison of Animal Discs Used in Disc Research to Human Lumbar Disc. Spine (Phila. Pa. 1976). 33, E166–E173. 10.1097/BRS.0b013e318166e001 [PubMed: 18344845]

Bongio M, van den Beucken JJJ, Nejadnik MR, Tahmasebi Birgani Z, Habibovic P, Kinard LA, Kasper FK, Mikos AG, Leeuwenburgh SCG, Jansen JA, 2013 Subcutaneous tissue response and osteogenic performance of calcium phosphate nanoparticle-enriched hydrogels in the tibial medullary cavity of guinea pigs. Acta Biomater. 9, 5464–74. 10.1016/j.actbio.2012.10.026 [PubMed: 23107797]

Bowles RD, Setton LA, 2017 Biomaterials for intervertebral disc regeneration and repair. Biomaterials 129, 54–67. 10.1016/j.biomaterials.2017.03.013 [PubMed: 28324865]

Buchbinder R, Blyth FM, March LM, Brooks P, Woolf AD, Hoy DG, 2013 Placing the global burden of low back pain in context. Best Pract. Res. Clin. Rheumatol 27, 575–589. 10.1016/j.berh.2013.10.007 [PubMed: 24315140]

Burke JG, Watson RWG, McCormack D, Dowling FE, Walsh MG, Fitzpatrick JM, 2002 Intervertebral discs which cause low back pain secrete high levels of proinflammatory mediators. J. Bone Jt. Surg 84, 196–201. 10.1302/0301-620X.84B2.12511

Cannella M, Isaacs JL, Allen S, Orana A, Vresilovic E, Marcolongo M, 2014 Nucleus Implantation: The Biomechanics of Augmentation Versus Replacement With Varying Degrees of Nucleotomy. J. Biomech. Eng 136, 51001 10.1115/1.4027056

Charron PN, Fenn SL, Poniz A, Oldinski RA, 2016 Mechanical properties and failure analysis of visible light crosslinked alginate-based tissue sealants. J. Mech. Behav. Biomed. Mater 59, 314–321. 10.1016/j.jmbbm.2016.02.003 [PubMed: 26897093]

Chou AI, Nicoll SB, 2009 Characterization of photocrosslinked alginate hydrogels for nucleus pulposus cell encapsulation. J. Biomed. Mater. Res. A 91, 187–94. 10.1002/jbm.a.32191 [PubMed: 18785646]

Cruz MA, Hom WW, DiStefano TJ, Merrill R, Torre OM, Lin HA, Hecht AC, Illien-Junger S, Iatridis JC, 2018 Cell-Seeded Adhesive Biomaterial for Repair of Annulus Fibrosus Defects in Intervertebral Discs. Tissue Eng. Part A 24, 187–198. 10.1089/ten.TEA.2017.0334 [PubMed: 29214889]

Demers CN, Antoniou J, Mwale F, 2004 Value and limitations of using the bovine tail as a model for the human lumbar spine. Spine (Phila. Pa. 1976). 29, 2793–9. [PubMed: 15599281]

Deng M, Nair LS, Nukavarapu SP, Jiang T, Kanner WA, Li X, Kumbar SG, Weikel AL, Krogman NR, Allcock HR, Laurencin CT, 2010 Dipeptide-based polyphosphazene and polyester blends for bone tissue engineering. Biomaterials 31, 4898–4908. 10.1016/j.biomaterials.2010.02.058 [PubMed: 20334909]

Dhillon N, Bass EC, Lotz JC, 2001 Effect of frozen storage on the creep behavior of human intervertebral discs. Spine (Phila Pa 1976). 26, 883–888. [PubMed: 11317110]

Di Martino A, Vaccaro AR, Lee JY, Denaro V, Lim MR, 2005 Nucleus Pulposus Replacement. Spine (Phila. Pa. 1976). 30, S16–S22. 10.1097/01.brs.0000174530.88585.32 [PubMed: 16103829]

Freemont a J., 2009 The cellular pathobiology of the degenerate intervertebral disc and discogenic back pain. Rheumatology (Oxford). 48, 5–10. 10.1093/rheumatology/ken396 [PubMed: 18854342]

Gleizes V, Viguier E, Féron JM, Canivet S, Lavaste F, 1998 Effects of freezing on the biomechanics of the intervertebral disc. Surg Radiol Anat. 20, 403–407. [PubMed: 9932324]

Goins ML, Wimberley DW, Yuan PS, Fitzhenry LN, Vaccaro AR, 2005 Nucleus pulposus replacement: an emerging technology. Spine J. 5, 317S–324S. 10.1016/j.spinee.2005.02.021 [PubMed: 16291129]

Griffith JF, Wang Y-XJ, Antonio GE, Choi KC, Yu A, Ahuja AT, Leung PC, 2007 Modified Pfirrmann Grading System for Lumbar Intervertebral Disc Degeneration. Spine (Phila. Pa. 1976). 32, E708–E712. 10.1097/BRS.0b013e31815a59a0 [PubMed: 18007231]

Gullbrand SE, Schaer TP, Agarwal P, Bendigo JR, Dodge GR, Chen W, Elliott DM, Mauck RL, Malhotra NR, Smith LJ, 2017 Translation of an injectable triple-interpenetrating-network hydrogel for intervertebral disc regeneration in a goat model. Acta Biomater. 60, 201–209. 10.1016/j.actbio.2017.07.025 [PubMed: 28735027]

Gupta MS, Cooper ES, Nicoll SB, 2011 Transforming Growth Factor-Beta 3 Stimulates Cartilage Matrix Elaboration by Human Marrow-Derived Stromal Cells Encapsulated in Photocrosslinked Carboxymethylcellulose Hydrogels: Potential for Nucleus Pulposus Replacement. Tissue Eng. Part A 17, 2903–2910. 10.1089/ten.tea.2011.0152 [PubMed: 21707438]

Haque A, Morris ER, 1993 Thermogelation of methylcellulose. Part I: molecular structures and processes. Carbohydr. Polym 22, 161–173. 10.1016/0144-8617(93)90137-S

Hedman TP, Kostuik JP, Fernie GR, Hellier WG, 1991 Design of an intervertebral disc prosthesis. Spine 16, S256–S260. [PubMed: 1862421]

Hoy D, March L, Brooks P, Woolf A, Blyth F, Vos T, Buchbinder R, 2010 Measuring the global burden of low back pain. Best Pract. Res. Clin. Rheumatol 24, 155–165. 10.1016/j.berh.2009.11.002 [PubMed: 20227638]

Iatridis JC, Nicoll SB, Michalek AJ, Walter BA, Gupta MS, 2013 Role of biomechanics in intervertebral disc degeneration and regenerative therapies: what needs repairing in the disc and what are promising biomaterials for its repair? Spine J. 13, 243–262. 10.1016/j.spinee.2012.12.002 [PubMed: 23369494]

Ibim SM, Uhrich KE, Bronson R, El-Amin SF, Langer RS, Laurencin CT, 1998 Poly(anhydride-co-imides): in vivo biocompatibility in a rat model. Biomaterials 19, 941–51. [PubMed: 9690836]

ISO-10993–6, 2008 International Standard 2005, 22674 10.5594/J09750

Kang JD, Georgescu HI, McIntyre-Larkin L, Stefanovic-Racic M, Donaldson WF, Evans CH, 1996 Herniated lumbar intervertebral discs spontaneously produce matrix metalloproteinases, nitric oxide, interleukin-6, and prostaglandin E2. Spine (Phila. Pa. 1976). 21, 271–7. [PubMed: 8742201]

Kastellorizios M, Tipnis N, Burgess DJ, 2015 Foreign Body Reaction to Subcutaneous Implants. Springer, Cham, pp. 93–108. 10.1007/978-3-319-18603-0_6

Katz JN, 2006 Lumbar disc disorders and low-back pain: socioeconomic factors and consequences. J. Bone Joint Surg. Am 88 Suppl 2, 21–4. 10.2106/JBJS.E.01273 [PubMed: 16595438]

Lasanianos NG, Triantafyllopoulos GK, Pneumaticos SG, 2015 Intervertebral Disc Herniation, in: Trauma and Orthopaedic Classifications. Springer London, London, pp. 243–245. 10.1007/978-1-4471-6572-9_54

Lee CK, 1988 Accelerated degeneration of the segment adjacent to a lumbar fusion. Spine (Phila. Pa. 1976). 13, 375–7. [PubMed: 3388124]

Lewis G, 2012 Nucleus pulposus replacement and regeneration/repair technologies: Present status and future prospects. J. Biomed. Mater. Res. Part B Appl. Biomater 100B, 1702–1720. 10.1002/jbm.b.32712

Li Z, Lang G, Chen X, Sacks H, Mantzur C, Tropp U, Mader KT, Smallwood TC, Sammon C, Richards RG, Alini M, Grad S, 2016 Polyurethane scaffold with in situ swelling capacity for nucleus pulposus replacement. Biomaterials 84, 196–209. 10.1016/j.biomaterials.2016.01.040 [PubMed: 26828684]

Likhitpanichkul M, Dreischarf M, Illien-Junger S, Walter BA, Nukaga T, Long RG, Sakai D, Hecht AC, Iatridis JC, 2014 Fibrin-genipin adhesive hydrogel for annulus fibrosus repair: performance evaluation with large animal organ culture, in situ biomechanics, and in vivo degradation tests. Eur. Cell. Mater 28, 25–37–8. [PubMed: 25036053]

Lin HA, Gupta MS, Varma DM, Gilchrist ML, Nicoll SB, 2016 Lower crosslinking density enhances functional nucleus pulposus-like matrix elaboration by human mesenchymal stem cells in carboxymethylcellulose hydrogels. J. Biomed. Mater. Res. A 104, 165–77. 10.1002/jbm.a.35552 [PubMed: 26256108]

Long RG, Bürki A, Zysset P, Eglin D, Grijpma DW, Blanquer SBG, Hecht AC, Iatridis JC, 2016a Mechanical restoration and failure analyses of a hydrogel and scaffold composite strategy for annulus fibrosus repair. Acta Biomater. 30, 116–125. 10.1016/j.actbio.2015.11.015 [PubMed: 26577987]

Long RG, Rotman SG, Hom WW, Assael DJ, Illien-Jünger S, Grijpma DW, Iatridis JC, 2017 In vitro and biomechanical screening of polyethylene glycol and poly(trimethylene carbonate) block copolymers for annulus fibrosus repair. J. Tissue Eng. Regen. Med 10.1002/term.2356

Long RG, Torre OM, Hom WW, Assael DJ, Iatridis JC, 2016b Design Requirements for Annulus Fibrosus Repair: Review of Forces, Displacements, and Material Properties of the Intervertebral Disk and a Summary of Candidate Hydrogels for Repair. J. Biomech. Eng 138, 21007 10.1115/1.4032353

Luoma K, Riihimäki H, Luukkonen R, Raininko R, Viikari-Juntura E, Lamminen A, 2000 Low back pain in relation to lumbar disc degeneration. Spine (Phila. Pa. 1976). 25, 487–92. [PubMed: 10707396]

McGirt MJ, Ambrossi GLG, Datoo G, Sciubba DM, Witham TF, Wolinsky J-P, Gokaslan ZL, Bydon A, 2009 Recurrent disc herniation and long-term back pain after primary lumbar discectomy. Neurosurgery 64, 338–345. 10.1227/01.NEU.0000337574.58662.E2 [PubMed: 19190461]

Miyamoto T, Takahashi S, Ito H, Inagaki H, Noishiki Y, 1989 Tissue biocompatibility of cellulose and its derivatives. J. Biomed. Mater. Res 23, 125–133. 10.1002/jbm.820230110 [PubMed: 2708402]

Nasatto P, Pignon F, Silveira J, Duarte M, Noseda M, Rinaudo M, 2015 Methylcellulose, a Cellulose Derivative with Original Physical Properties and Extended Applications. Polymers (Basel). 7, 777–803. 10.3390/polym7050777

Neidlinger-Wilke C, Galbusera F, Pratsinis H, Mavrogonatou E, Mietsch A, Kletsas D, Wilke H-J, 2014 Mechanical loading of the intervertebral disc: from the macroscopic to the cellular level. Eur. Spine J 23, 333–343. 10.1007/s00586-013-2855-9

O'Brien FJ, 2011 Biomaterials & scaffolds for tissue engineering. Mater. Today 14, 88–95. 10.1016/S1369-7021(11)70058-X

O'Connell GD, Vresilovic EJ, Elliott DM, 2007 Comparison of Animals Used in Disc Research to Human Lumbar Disc Geometry. Spine (Phila. Pa. 1976). 32, 328–333. 10.1097/01.brs.0000253961.40910.c1 [PubMed: 17268264]

Olmarker K, Rydevik B, 1998 New information concerning pain caused by herniated disk and sciatica. Exposure to disk tissue sensitizes the nerve roots. Lakartidningen 95, 5618–22. [PubMed: 9863299]

Onuki Y, Bhardwaj U, Papadimitrakopoulos F, Burgess DJ, 2008 A review of the biocompatibility of implantable devices: current challenges to overcome foreign body response. J. Diabetes Sci. Technol 2, 1003–15. 10.1016/S0091-679X(07)83003-2 [PubMed: 19885290]

Ordway NR, Lavelle WF, Brown T, Bin Bao, Q., 2013 Biomechanical assessment and fatigue characteristics of an articulating nucleus implant. Int. J. Spine Surg 7, e109–e117. 10.1016/j.ijsp.2013.10.001 [PubMed: 25694897]

Oshima H, Ishihara H, Urban JPG, Tsuji H, 1993 The use of coccygeal discs to study intervertebral disc metabolism. J. Orthop. Res 11, 332–338. 10.1002/jor.1100110304 [PubMed: 8326439]

Park P, Garton HJ, Gala VC, Hoff JT, McGillicuddy JE, 2004 Adjacent segment disease after lumbar or lumbosacral fusion: review of the literature. Spine (Phila. Pa. 1976). 29, 1938–44. [PubMed: 15534420]

Parker SL, Grahovac G, Vukas D, Vilendecic M, Ledic D, McGirt MJ, Carragee EJ, 2016 Effect of an Annular Closure Device (Barricaid) on Same-Level Recurrent Disk Herniation and Disk Height Loss After Primary Lumbar Discectomy: Two-year Results of a Multicenter Prospective Cohort Study. Clin. spine Surg 29, 454–460. 10.1097/BSD.0b013e3182956ec5 [PubMed: 27879508]

Pfirrmann CW, Metzdorf A, Zanetti M, Hodler J, Boos N, 2001 Magnetic resonance classification of lumbar intervertebral disc degeneration. Spine (Phila. Pa. 1976). 26, 1873–8. [PubMed: 11568697]

Raj PP, 2008 Intervertebral disc: anatomy-physiology-pathophysiology-treatment. Pain Pract. 8, 18–44. 10.1111/j.1533-2500.2007.00171.x [PubMed: 18211591]

Reza AT, Nicoll SB, 2010 Characterization of novel photocrosslinked carboxymethylcellulose hydrogels for encapsulation of nucleus pulposus cells. Acta Biomater. 6, 179–86. 10.1016/j.actbio.2009.06.004 [PubMed: 19505596]

Risbud MV, 2014 The Intervertebral Disc. Springer Vienna, Vienna 10.1007/978-3-7091-1535-0

Roberts S, Menage J, Sivan S, Urban JPG, 2008 Bovine explant model of degeneration of the intervertebral disc. BMC Musculoskelet. Disord 9, 24 10.1186/1471-2474-9-24 [PubMed: 18298830]

Roughley PJ, 2004 Biology of intervertebral disc aging and degeneration: involvement of the extracellular matrix. Spine (Phila. Pa. 1976). 29, 2691–9. [PubMed: 15564918]

Schmocker A, Khoushabi A, Frauchiger D. a., Gantenbein B, Schizas C, Moser C, Bourban PE, Pioletti DP, 2016 A photopolymerized composite hydrogel and surgical implanting tool for a nucleus pulposus replacement. Biomaterials 88, 110–119. 10.1016/j.biomaterials.2016.02.015 [PubMed: 26976264]

Schnake KJ, Putzier M, Haas NP, Kandziora F, 2006 Mechanical concepts for disc regeneration. Eur. Spine J 15, 354–360. 10.1007/s00586-006-0176-y

Schwarzer AC, Aprill CN, Derby R, Fortin J, Kine G, Bogduk N, 1995 The prevalence and clinical features of internal disc disruption in patients with chronic low back pain. Spine (Phila. Pa. 1976). 20, 1878–83. [PubMed: 8560335]

Showalter BL, Beckstein JC, Martin JT, Beattie EE, Espinoza Orías AA, Schaer TP, Vresilovic EJ, Elliott DM, 2012 Comparison of animal discs used in disc research to human lumbar disc: torsion mechanics and collagen content. Spine (Phila. Pa. 1976). 37, E900–7. 10.1097/BRS.0b013e31824d911c [PubMed: 22333953]

Showalter BL, Elliott DM, Chen W, Malhotra NR, 2015 Evaluation of an In Situ Gelable and Injectable Hydrogel Treatment to Preserve Human Disc Mechanical Function Undergoing

Physiologic Cyclic Loading Followed by Hydrated Recovery. J. Biomech. Eng 137, 81008 10.1115/1.4030530

Showalter BL, Malhotra NR, Vresilovic EJ, Elliott DM, 2014 Nucleotomy reduces the effects of cyclic compressive loading with unloaded recovery on human intervertebral discs. J. Biomech 47, 2633–40. 10.1016/j.jbiomech.2014.05.018 [PubMed: 24957922]

Smeathers JE, Joanes DN, 1988 Dynamic compressive properties of human lumbar intervertebral joints: A comparison between fresh and thawed specimens. J. Biomech 21, 425–433. [PubMed: 3417694]

Smith LJ, Gorth DJ, Showalter BL, Chiaro JA, Beattie EE, Elliott DM, Mauck RL, Chen W, Malhotra NR, 2014 In Vitro Characterization of a Stem-Cell-Seeded Triple-Interpenetrating-Network Hydrogel for Functional Regeneration of the Nucleus Pulposus. Tissue Eng. Part A 20, 1841–1849. 10.1089/ten.tea.2013.0516 [PubMed: 24410394]

Subramanian A, Krishnan UM, Sethuraman S, 2013 In vivo biocompatibility of PLGA-polyhexylthiophene nanofiber scaffolds in a rat model. Biomed Res. Int 2013, 390518 10.1155/2013/390518 [PubMed: 23971031]

Suk KS, Lee HM, Moon SH, Kim NH, 2001 Recurrent lumbar disc herniation: results of operative management. Spine (Phila. Pa. 1976). 26, 672–6. [PubMed: 11246384]

Urban JP, Roberts S, 2003 Degeneration of the intervertebral disc. Arthritis Res. Ther 5, 120 10.1186/ar629 [PubMed: 12723977]

Varma DM, Lin HA, Long RG, Gold GT, Hecht AC, Iatridis JC, Nicoll SB, 2018a Thermoresponsive, redox-polymerized cellulosic hydrogels undergo in situ gelation and restore intervertebral disc biomechanics post discectomy. Eur. Cells Mater 35, 300–317. 10.22203/eCM.v035a21

Varma DM, DiNicolas MS, Nicoll SB, 2018b Injectable, redox-polymerized carboxymethylcellulose hydrogels promote nucleus pulposus-like extracellular matrix elaboration by human MSCs in a cell density-dependent manner. J. Biomater. Appl 33, 576–589. [PubMed: 30326804]

Vergroesen P.-P. a., Bochyńska AI, Emanuel KS, Sharifi S, Kingma I, Grijpma DW, Smit TH, 2015 A Biodegradable Glue for Annulus Closure. Spine (Phila. Pa. 1976). 40, 622–628. 10.1097/BRS.0000000000000792 [PubMed: 25608249]

Vital JM, Boissière L, 2014 Total disc replacement. Orthop. Traumatol. Surg. Res 100, S1–14. 10.1016/j.otsr.2013.06.018 [PubMed: 24412045]

Walter BA, Illien-Jünger S, Nasser PR, Hecht AC, Iatridis JC, 2014 Development and validation of a bioreactor system for dynamic loading and mechanical characterization of whole human intervertebral discs in organ culture. J. Biomech 47, 2095–2101. 10.1016/j.jbiomech.2014.03.015 [PubMed: 24725441]

Whatley BR, Wen X, 2012 Intervertebral disc (IVD): Structure, degeneration, repair and regeneration. Mater. Sci. Eng. C 32, 61–77. 10.1016/j.msec.2011.10.011

Wilke HJ, Ressel L, Heuer F, Graf N, Rath S, 2013 Can prevention of a reherniation be investigated? Establishment of a herniation model and experiments with an anular closure device. Spine (Phila. Pa. 1976). 38, E587–93. 10.1097/BRS.0b013e31828ca4bc [PubMed: 23429676]

Yorimitsu E, Chiba K, Toyama Y, Hirabayashi K, 2001 Long-term outcomes of standard discectomy for lumbar disc herniation: a follow-up study of more than 10 years. Spine (Phila. Pa. 1976). 26, 652–7. [PubMed: 11246379]

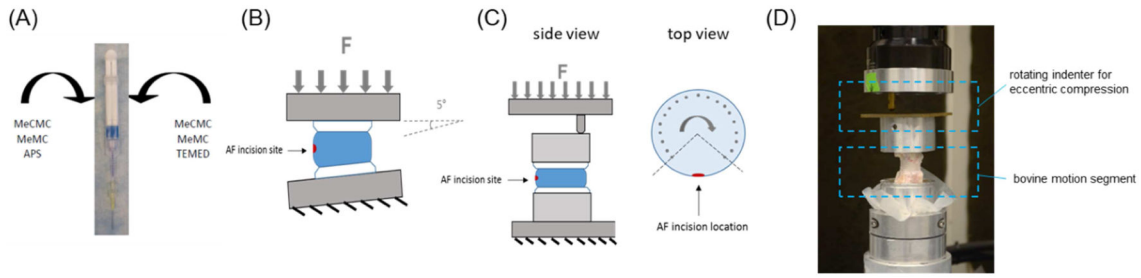

Figure 1:

Hydrogel preparation and motion segment testing schematics: (A) CMC-MC hydrogel was delivered via a dual-barrel syringe with a mixing tip and an attached 20G needle; (B) herniation risk was determined by failure testing which consisted of displacement-controlled compression at 5° angle; (C) fatigue endurance was assessed by fatigue testing which consisted of cyclic eccentric compression using an indenter while specimen was under rotation (top view schematic indicates loading points); and (D) photograph of fatigue testing setup.

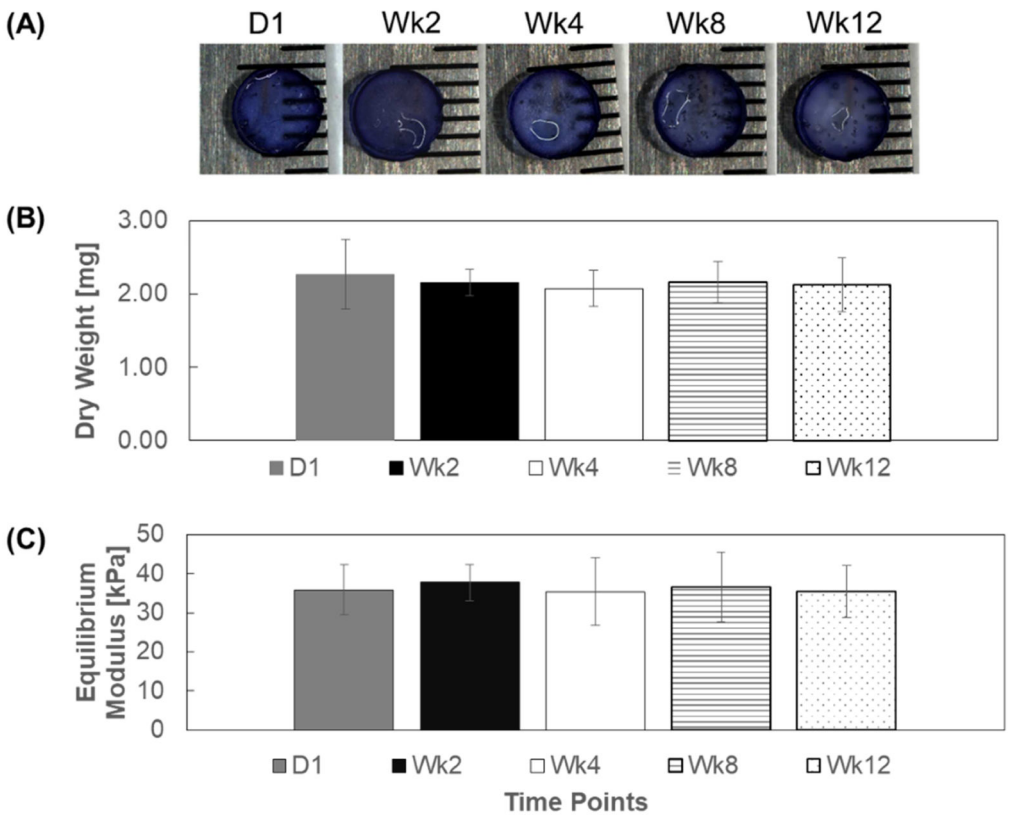

Figure 2:

In vitro gel structural stability: (A) representative gel image from each time point (B) dry weight and (C) equilibrium moduli of CMC-MC hydrogels over a 12-week period.

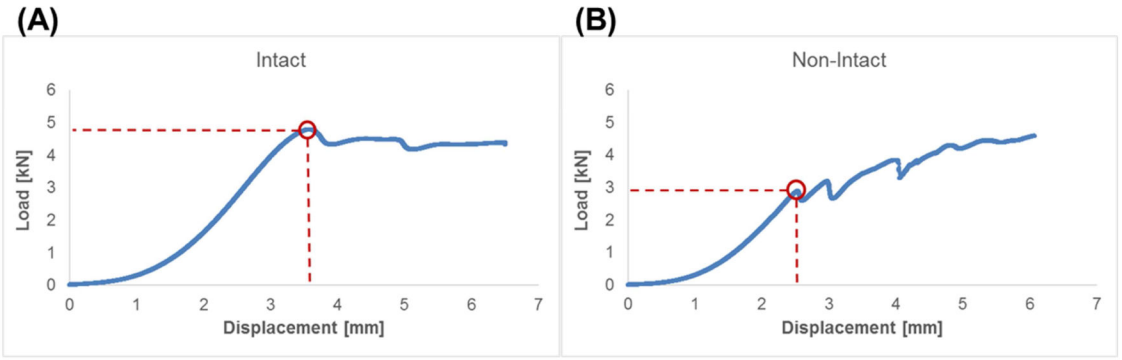

Figure 3:

Representative load-displacement curves for (A) Intact samples indicative of endplate fracture and (B) non-Intact (Injury, Nucleotomy, and Repair) samples indicative of nuclear extrusion. Red circle indicate point of failure.

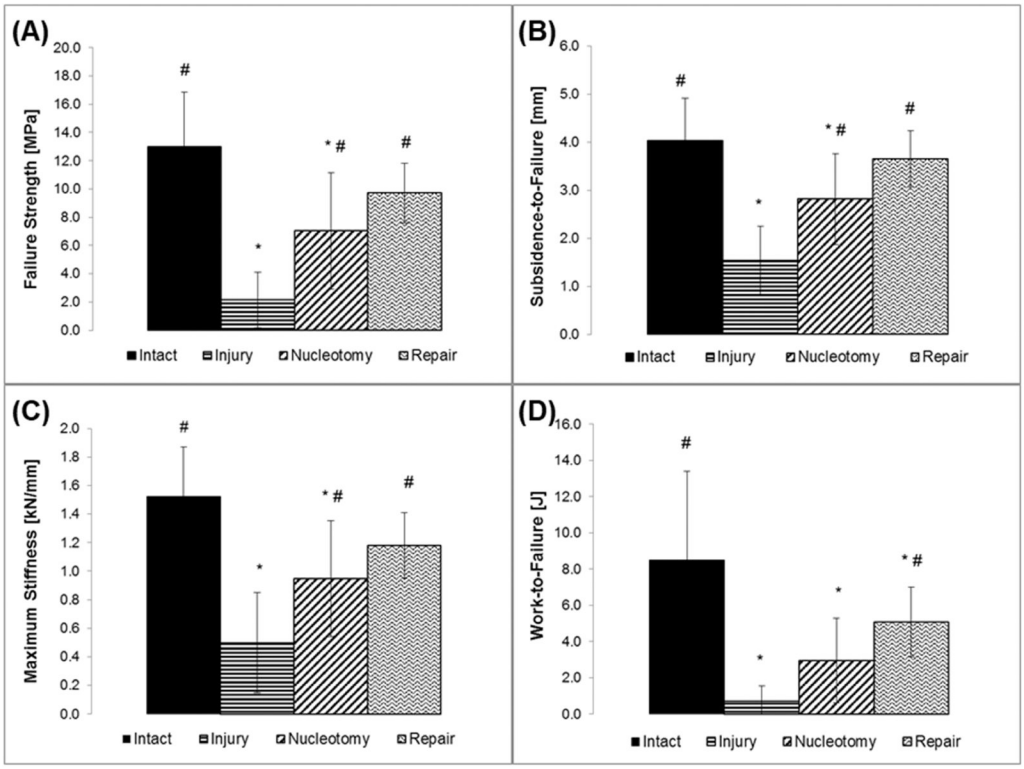

Figure 4:

Outcome measures from failure testing indicative of herniation risk: (A) failure strength, (B) subsidence-to-failure, (C) maximum stiffness, and (D) work-to-failure. # - significantly different from the Injury group. * - significantly different from the Intact group.

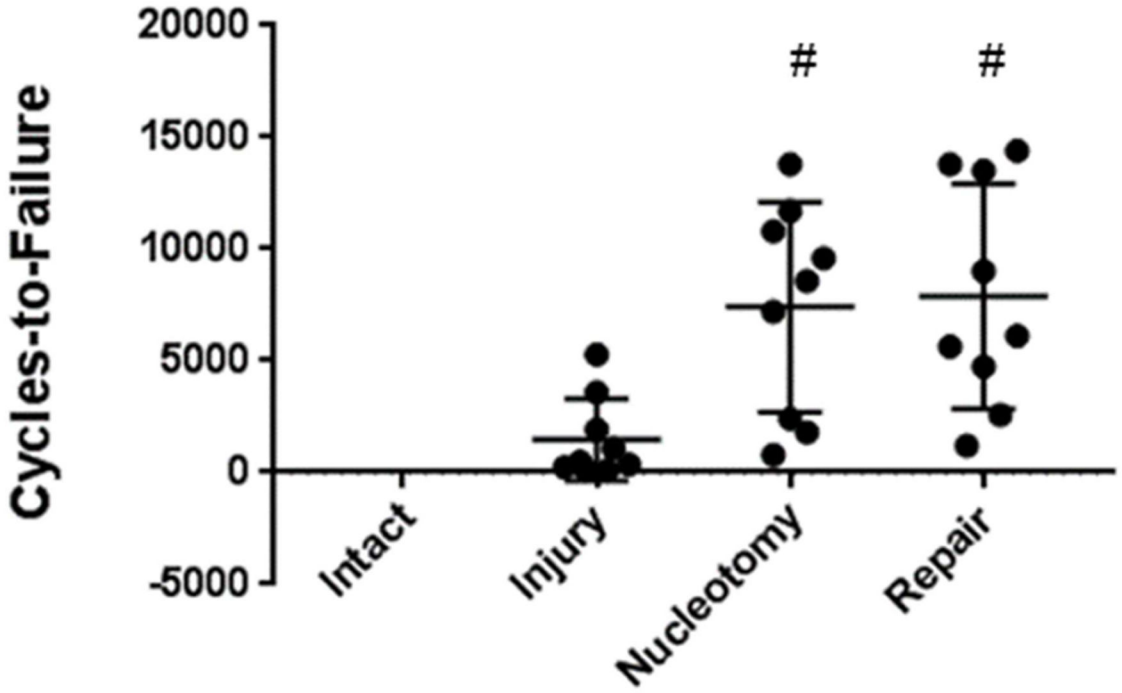

Figure 5:
Cycles-to-failure results from fatigue testing. Intact group did not fail during the test of 21,000 cycles. # - significantly different from the Injury group.

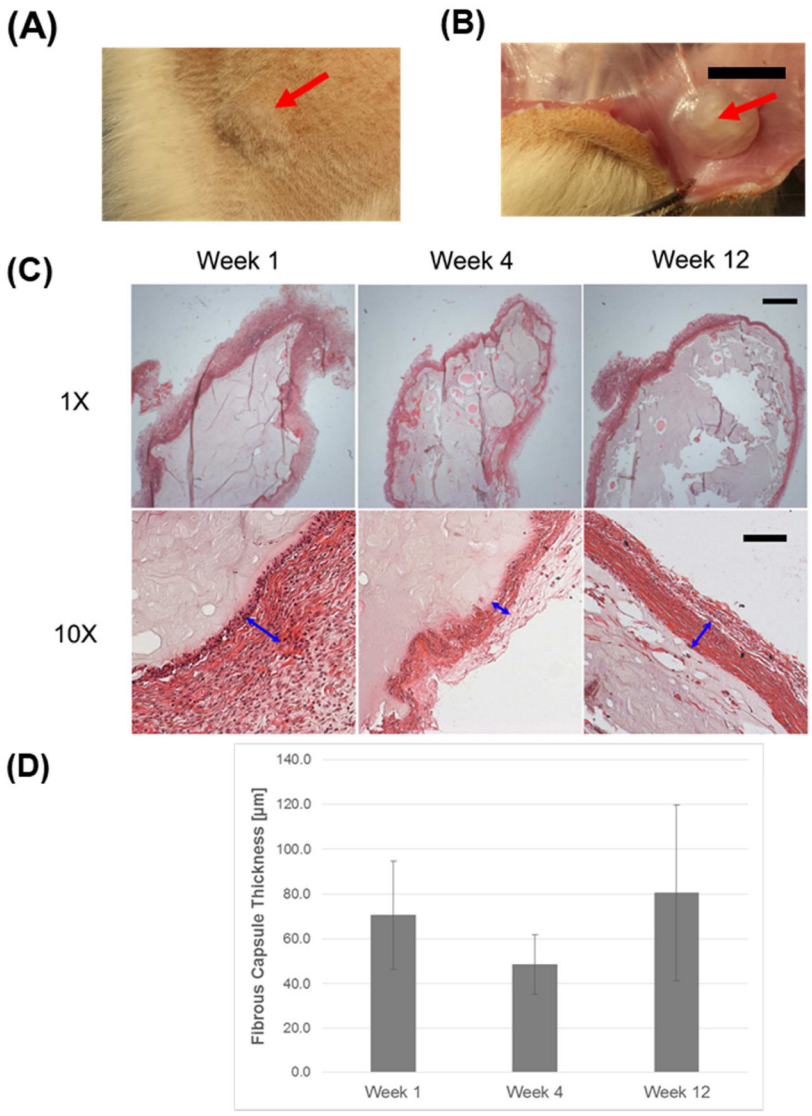

Figure 6:

In vivo biocompatibility results: (A) CMC-MC hydrogels maintained structural integrity over 12 weeks in vivo in rat subcutaneous dorsa, with a visual bump indicating the presence of the injected hydrogel, and (B) a representative gross image of an extracted gel at week 12. (C) Representative H&E images of extracted CMC-MC hydrogels showing the presence of a histiocytic reaction and the development of a fibrous capsule. (D) Fibrous capsule thicknesses were not significantly different across the three time points. Red arrows point to the CMC-MC hydrogels in (A), (B). Blue arrows indicate the fibrous capsule thicknesses in (C). Scale bar = 10 mm for (B); 1000 μm for 1X magnification images; and 100 μm for 10X magnification images in (C).

(A)

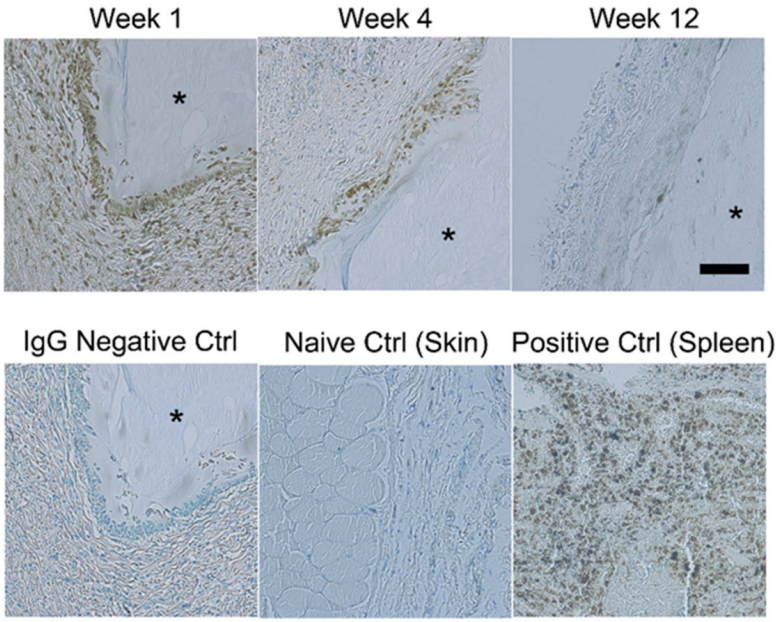

(B)

	Rat#1	Rat#2	Rat#3	Rat#4	Rat#5	Rat#6	Rat#7	Rat#8	Rat#9
Week 1	++	++	++	++	++	++	++	++	++
Week 4	++	++	+	++	++	++	+	+	++
Week 12	+	+	+	+	+	+	+	+	+

Figure 7:

In vivo biocompatibility results: (A) Representative CD68 immunostaining of extracted gels at week 1, 4, and 12, along with IgG negative control, skin naïve control, and spleen positive control, showing decreased CD68+ macrophage presence over time. (B) Grading chart of CD68+ macrophage presence indicating marked subsidence from moderate presence at week 1 to mild presence at week 12. * - denotes gel location. Scale bar = 100 μm